

COMBINING RESAMPLING AND REWEIGHTING FOR FAITHFUL STOCHASTIC OPTIMIZATION

JING AN AND LEXING YING

ABSTRACT. Many machine learning and data science tasks require solving non-convex optimization problems. When the loss function is a sum of multiple terms, a popular method is stochastic gradient descent. Viewed as a process for sampling the loss function landscape, the stochastic gradient descent is known to prefer flat local minimums. Though this is desired for certain optimization problems such as in deep learning, it causes issues when the goal is to find the global minimum, especially if the global minimum resides in a sharp valley.

Illustrated with a simple motivating example, we show that the fundamental reason is that the difference in the Lipschitz constants of multiple terms in the loss function causes stochastic gradient descent to experience different variances at different minimums. In order to mitigate this effect and perform faithful optimization, we propose a combined resampling-reweighting scheme to balance the variance at local minimums and extend to general loss functions. We also explain from the stochastic asymptotics perspective how the proposed scheme is more likely to select the true global minimum when compared with the vanilla stochastic gradient descent. Experiments from robust statistics, computational chemistry, and neural network training are provided to demonstrate the theoretical findings.

1. INTRODUCTION

This paper is concerned with optimizing a non-convex smooth loss function. Identifying a global minimum is known to be computationally hard, especially in the high-dimensional setting. One possible approach, originated from early work in statistical mechanics and Monte Carlo methods, is to turn this into the task of sampling approximately the Gibbs distribution associated with the loss function at a sufficiently low temperature. The rationale is that the samples from the Gibbs distribution have a good chance of being near the global minimum.

In modern machine learning, the loss function often takes the form of an empirical sum of individual terms from finitely many sampled data points. Due to the large size of the dataset, efficient optimization methods such as the stochastic gradient descent (SGD) are commonly used. For non-convex loss function, an increasingly more popular viewpoint is to consider SGD as a sampling algorithm.

One important feature of stochastic gradient-type algorithms is that the noise drives SGD to escape from sharp minimums quickly and hence SGD prefers flat minimums [25, 22, 7, 24, 20]. Such a bias towards flat minimums leads to better generalization properties for problems such as deep learning. However, when the ultimate goal is to identify the global minimum and the landscape around the global minimum happens to be sharper compared to the non-global local minima, this bias is often not desired as SGD often misses the global minimum in a sharp valley.

In fact for both many science and physical science problems, the ultimate goal is to find the global minimum for a non-convex landscape, independent of whether it is sharp or flat. In data sciences, one example is the handling of contaminated data, where a simple approach is to use non-convex loss functions in robust statistics [15, 19, 8, 2]. However, as we shall see later in an example, if we naively apply the vanilla stochastic gradient over a dataset comprised of two types of patterns, where one group has much larger features (more sensitive) compared to the other (less sensitive), the resulted optimal parameter will be biased towards the less sensitive

The work of L.Y. is partially supported by the U.S. Department of Energy, Office of Science, Office of Advanced Scientific Computing Research, Scientific Discovery through Advanced Computing (SciDAC) program and also by the National Science Foundation under award DMS-1818449. J.A. is supported by Joe Olinger Fellowship from Stanford University.

group. This scenario is not rare in real applications: for example, when researchers adjust a medicine’s ingredients by evaluating the tested group’s responses, inherently different hormone levels in individuals can affect the faithfulness of the evaluation. In physical sciences, examples of non-convex global minimization include finding the ground state wave function in quantum many body problems [11], geometry optimization of the potential energy surface of a molecule in computational chemistry [12], and etc. Though applying vanilla stochastic gradient can reduce computational cost for these large scale problems, one also takes the risk of missing the global minimum.

Main contributions. Below we summarize the main contributions of this paper.

- (1) Starting from a motivating example, we identify the fundamental reason behind the selection bias is that the difference in the Lipschitz constants of multiple terms in the loss function causes stochastic gradient descent to experience different variances at different local minimums.
- (2) To mitigate the bias, we propose a combined resampling-reweighting strategy for faithful minimum selections. We also derive stochastic differential equation (SDE) models to shed lights on how the proposed strategy balances variances in different regions. This proposed strategy also recovers the importance sampling SGD for faster training (for example, [23, 10]) from a different perspective.
- (3) We show also empirically that the proposed strategy outperforms SGD with examples from robust statistics, computational chemistry, and neural network training.

Related work. Our proposed combined resampling-reweighting strategy can be viewed as a form of importance sampling. This line of works can be traced back to the randomized Kaczmarz method [21] that selects rows with probability proportional to their squared norms. Later, [18] connects the randomized Kaczmarz method with a SGD algorithm with importance sampling. In convex optimization, many works [18, 23, 3] show that the importance sampling among stochastic gradients can improve the convergence speed. Since importance sampling reduces the stochastic gradient’s variance, this method and its variants can also accelerate the neural networks training [1, 9, 14, 10]. However, it has not been studied yet that how the importance sampling impacts the minimum selection in the learning.

Taking the continuous-time limit and using SDEs to analyze stochastic algorithms have become popular especially for stochastic non-convex problems. Using the developed stochastic analysis can lead to numerous new insights of the non-convex optimization [13, 4, 16, 5]. Here we take the SDE approximation approach as it gives us a clearer picture of the global minimum selection.

2. MAIN IDEA FROM A MOTIVATING EXAMPLE

Given a dataset consisting of n samples $\{x_i\}_{i=1}^n$, we consider an optimization problem

$$\min_{\theta} \frac{1}{n} \sum_{i=1}^n V(x_i, \theta).$$

The samples are assumed to come from m different subgroups, each representing a proportion $a_j \in (0, 1)$ of the overall population, i.e., $\sum_{j=1}^m a_j = 1$. Assuming that loss term $V(x_i, \theta)$ only depends on the subgroup index of x_i , i.e., $V(x_i, \theta) = V_j(\theta)$ if x_i is from subgroup j , the optimization problem can be simplified as

$$(1) \quad \theta^* = \operatorname{argmin}_{\theta} V(\theta), \quad V(\theta) \equiv \sum_{j=1}^m a_j V_j(\theta),$$

in the large n limit. If the terms $V_j(\theta)$ are non-convex loss functions, the overall loss function $V(\theta)$ is in general non-convex as well. From the next example, we will show that applying the vanilla SGD to solve (1) becomes problematic when V_j ’s exhibit drastically different Lipschitz constants. An illustrative example. Consider the case of two subgroups with the following loss functions,

$$V_1(\theta) = \begin{cases} |\theta + 1| - 1, & \theta \leq 0 \\ \epsilon\theta, & \theta > 0 \end{cases}, \quad V_2(\theta) = \begin{cases} -\epsilon\theta, & \theta \leq 0 \\ |K\theta - 1| - 1, & \theta > 0 \end{cases}$$

with $\epsilon \in (0, 1)$ small and $K > 0$. The total loss function is $V(\theta) = a_1 V_1(\theta) + a_2 V_2(\theta)$ with local minimums $\theta = -1$ and $\theta = 1/K$. By construction, the loss function has a sharp global minimum and a flat local minimum (see for example Fig 1 (1)). Without loss of generality, we assume that $K > 1$ and $a_2 > a_1$ so that the sharp global minimum lies at $\theta = 1/K$.¹

The following lemma states that the optimization trajectory of the vanilla SGD is biased towards one of the local minimum, in the small learning rate η limit.

Lemma 1. *When η is sufficiently small, the equilibrium distribution of the vanilla SGD is given given by*

$$p(\theta) \sim \begin{cases} \exp\left(-\frac{2}{a_1 a_2 \eta} V(\theta)\right) & \text{for } \theta < 0, \\ \frac{1}{K^2} \exp\left(-\frac{2}{K^2 a_1 a_2 \eta} V(\theta)\right) & \text{for } \theta > 0, \end{cases}$$

up to a normalizing constant.

The derivation follows from approximating the SGD updates by an SDE with a numerical error of order $O(\sqrt{\eta})$ in the weak sense. Because the loss function considered is piece-wise linear, the approximate SDEs are of Langevin dynamics form with piecewise constant noise coefficients. In particular, when the dynamics reaches equilibrium, the stationary distribution of the stochastic process can be approximated by a Gibbs distribution. The detailed computations of Lemma 1 is given in the Appendix A.

From Lemma 1, we can make the following surprising observation: *When $K \gg 1$, even though $\theta = 1/K$ is the global minimum, the SGD trajectory spends most of the time near the non-global local minimum $\theta = -1$.* This is illustrated in Figure 1(2) and the fundamental reason is that the Lipschitz constant of the individual loss term affects the SGD variance at individual local minimum, thus resulting undesired equilibrium distribution.

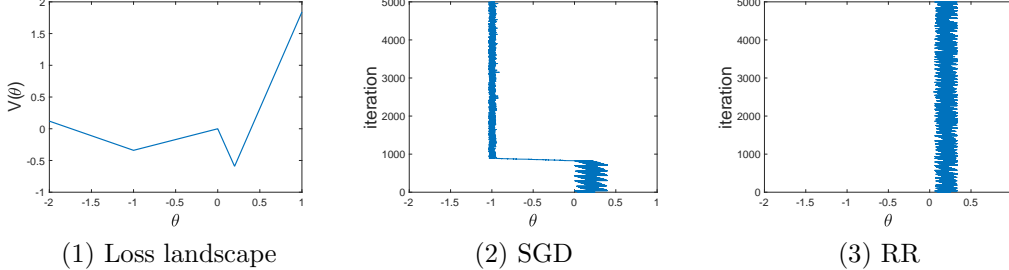


FIGURE 1. We set $a_1 = 0.4$, $a_2 = 0.6$, $\epsilon = 0.1$, $K = 5$ so that the global minimum is at $\theta = 1/5$. For both the vanilla SGD and the resampling-reweighting (RR) scheme, we start from $\theta_0 = 0.25$ and use a fixed step size $\eta = 0.04$. We can see that the vanilla SGD jumps to the non-global local minimum $\theta = -1$ after several iterations while the RR method stays around the global minimum $\theta = 1/K$ all the time. We include more comparisons with various learning rates in the Appendix C to show that the RR scheme is stable for a wider range of η .

To fix this issue, we propose to *resample* two subgroups with proportion f_1 and f_2 , respectively (with $f_1, f_2 > 0$, $f_1 + f_2 = 1$). In order to maintain the same overall loss function, we also need to *reweight* each loss term with weights $w_1 := a_1/f_1, w_2 := a_2/f_2 > 0$. The values of f_1, f_2, w_1 , and w_2 are to be determined depending on a_1, a_2 and K . After reweighting and resampling, the loss function can be reformulated equivalently as

$$(2) \quad V(\theta) = f_1 \cdot \left(\frac{a_1}{f_1} V_1(\theta)\right) + f_2 \cdot \left(\frac{a_2}{f_2} V_2(\theta)\right).$$

¹It is necessary to have $O(\epsilon)$ terms in the loss function for SGD to work. Without the $O(\epsilon)$ terms, if the SGD starts in $(-\infty, 0)$ it will stay in this region because there is no drift from $V_2(x)$. Similarly, if the SGD starts in $(0, \infty)$, it will stay in this region. That means the result of SGD only depends on the initialization when $O(\epsilon)$ term is missing.

In each iteration, a data point is then sampled from the two groups following proportion f_1 and f_2 and either $\frac{a_1}{f_1}V_1(\theta)$ or $\frac{a_2}{f_2}V_2(\theta)$ is used for computing the stochastic gradient. In what follows, we refer to this approach as the *resampling-reweighting* (RR) scheme.

Although under the expectation of the stochastic gradients in (2) remains the same by design, the variance experienced in different regions now can be balanced by the parameters f_1, f_2 . A direct computation shows that in the four regions $(-\infty, -1)$, $(-1, 0)$, $(0, 1/K)$, and $(1/K, \infty)$

- With probability f_1 , the gradients are $-a_1/f_1, a_1/f_1, \epsilon a_1/f_1, \epsilon a_1/f_1$ respectively.
- With probability f_2 , the gradients are $-\epsilon a_2/f_2, -\epsilon a_2/f_2, -K a_2/f_2, K a_2/f_2$ respectively.
- The variances of the gradients are equal to $\left(a_1\sqrt{\frac{f_2}{f_1}} - \epsilon a_2\sqrt{\frac{f_1}{f_2}}\right)^2, \left(a_1\sqrt{\frac{f_2}{f_1}} + \epsilon a_2\sqrt{\frac{f_1}{f_2}}\right)^2, \left(\epsilon a_1\sqrt{\frac{f_2}{f_1}} + K a_2\sqrt{\frac{f_1}{f_2}}\right)^2, \left(\epsilon a_1\sqrt{\frac{f_2}{f_1}} - K a_2\sqrt{\frac{f_1}{f_2}}\right)^2$, respectively.

The dynamics of RR becomes straightforward if we view it as a numerical approximation of SDEs: with a sufficiently small step size $\eta > 0$, taking $\epsilon \rightarrow 0$, it is given by

$$\begin{aligned} d\Theta_t &= -V'(\Theta_t)dt + a_1\sqrt{f_2/f_1}\sqrt{\eta}dW_t, & \text{in the region } \theta < 0, \\ d\Theta_t &= -V'(\Theta_t)dt + K a_2\sqrt{f_1/f_2}\sqrt{\eta}dW_t, & \text{in the region } \theta > 0. \end{aligned}$$

In order to balance the variance at the two local minima $\theta = -1$ and $\theta = 1/K$, we impose

$$a_1\sqrt{f_2/f_1} = K a_2\sqrt{f_1/f_2} \implies f_1 = \frac{a_1}{a_1 + K a_2}, \quad f_2 = 1 - f_1 = \frac{K a_2}{a_1 + K a_2}.$$

As a result, the assigned weights for the two subgroups are

$$w_1 := \frac{a_1}{f_1} = \frac{a_1 + K a_2}{1}, \quad w_2 := \frac{a_2}{f_2} = \frac{a_1 + K a_2}{K}.$$

The above computation suggests that in order to fix the selection bias, each subgroup should be reweighted by the reciprocal of its Lipschitz constant. We then undersample data samples of pattern 1 and oversample data samples of pattern 2 so that their sample size ratio approaches $K a_2/a_1$. In numerical tests, comparing Fig 1 (2) and (3), we can see that the RR scheme adjusts the dynamics of the stochastic optimization trajectory to stay around the global minimum.

3. GENERAL CASE AND SDE ANALYSIS

In this section, we consider the general empirical loss for $\theta \in \mathbb{R}^d, d \geq 1$.

$$(3) \quad L(\theta) = \frac{1}{n} \sum_{i=1}^n l_i(\theta).$$

The general RR scheme. Motivated by the illustrative example, we propose the following resampling-reweighting scheme. At each k -th iteration with current parameter θ^k , for each term $i = 1, 2, \dots, n$,

- (1) Reweight the i -th term $l_i(\theta^k)$ with a weight proportional to $1/\|\nabla l_i(\theta^k)\|_2$,
- (2) Set the resampling probability for the (reweighted) i -th term to $\|\nabla l_i(\theta^k)\|_2$.

Recomputing the weights and sampling proportions in each iteration is obviously expensive. In practice, because of the continuity of the training trajectory, we can get away with computing these quantities and reusing for multiple iterations (for example, every 100 iterations). Numerically, this still gives rise to good training results.

The resampling proportions and weights are found when comparing the RR scheme with SGD in the continuous-time limit. More specifically, since the proposed RR scheme is designed for variance-balancing, in the SDE limit it should share the same drift with the vanilla SGD but experience more balanced noises across different local minimums.

SGD Derivations. For the vanilla SGD, the update rule with time step size $\eta > 0$ is given by

$$(4) \quad \theta^{k+1} = \theta^k - \eta \nabla l_j(\theta^k),$$

where the index j is chosen from 1 to n with uniform probability $1/n$. Note that

$$(5) \quad m(\theta^k) = \mathbb{E}_{p_1}[\nabla l_i(\theta^k)] = \frac{1}{n} \sum_{i=1}^n \nabla l_i(\theta^k) = \nabla L(\theta^k),$$

and we can rewrite (4) as

$$\theta^{k+1} = \theta^k - \eta m(\theta^k) + \sqrt{\eta} V^1(\theta^k), \quad \text{with } V^1(\theta^k) = \sqrt{\eta} (m(\theta^k) - \nabla l_j(\theta^k)).$$

By taking the simplifying assumption that the gradient noise is Gaussian², the dynamics can be approximated by

$$(6) \quad d\Theta_t = -m(\Theta_t)dt + \sqrt{\eta} \sigma^1(\Theta_t) dW_t,$$

where $\Sigma^1(\Theta_t) := \sigma^1(\Theta_t) \sigma^1(\Theta_t)^\top$ is given by $\Sigma^1(\Theta_t) = \frac{1}{n} \sum_{i=1}^n \nabla l_i(\Theta_t) \nabla l_i(\Theta_t)^\top - m(\Theta_t) \otimes^2$.

The RR scheme with the same time step size $\eta > 0$ is given by

$$(7) \quad \theta^{k+1} = \theta^k - \eta \frac{C(\theta^k)}{\|\nabla l_j(\theta^k)\|_2} \nabla l_j(\theta^k).$$

Here $C(\theta^k) = \frac{1}{n} \sum_{i=1}^n \|\nabla l_i(\theta^k)\|_2$ as indicated in the illustrative example and the index j is chosen from 1 to n with probability $\|\nabla l_i(\theta^k)\|_2 / Z(\theta^k)$, with the normalizing factor $Z(\theta^k) = \sum_{i=1}^n \|\nabla l_i(\theta^k)\|_2$, so that the mean for this approach matches with the one for SGD (5),

$$\sum_{i=1}^n \frac{C(\theta^k)}{\|\nabla l_i(\theta^k)\|_2} \nabla l_i(\theta^k) \frac{\|\nabla l_i(\theta^k)\|_2}{Z(\theta^k)} = \frac{1}{n} \sum_{i=1}^n \nabla l_i(\theta^k) = m(\theta^k).$$

Now we rewrite (7) in the form

$$\theta^{k+1} = \theta^k - \eta m(\theta^k) + \sqrt{\eta} V^2(\theta^k), \quad \text{with } V^2(\theta^k) = \sqrt{\eta} \left(m(\theta^k) - \frac{C(\theta^k)}{\|\nabla l_j(\theta^k)\|_2} \nabla l_j(\theta^k) \right).$$

Thus, the resulted dynamics can be approximated as

$$(8) \quad d\Theta_t = -m(\Theta_t)dt + \sqrt{\eta} \sigma^2(\Theta_t) dW_t,$$

where $\Sigma^2(\Theta_t) = \sigma^2(\Theta_t) \sigma^2(\Theta_t)^\top$ is given by $\Sigma^2(\Theta_t) = \frac{Z(\Theta_t)}{n^2} \sum_{i=1}^n \frac{\nabla l_i(\Theta_t) \nabla l_i(\Theta_t)^\top}{\|\nabla l_i(\Theta_t)\|_2} - m(\Theta_t) \otimes^2$.

Since (6) and (8) are derived in the same time scale and have the same drift, we analyze their different behaviors simply by comparing the noise terms.

Remark 1. The RR scheme (7) from the derivation turns out to be similar to [23] for faster convergence of regularized convex minimization problems, [10] for training deep learning with importance sampling, and even [21] for solving linear systems of equations earlier on.

Convergence to a local minimum. We can leverage the tools from stochastic calculus to give a compact estimate of the local convergence speed. We make the following remark as when computing the convergence rate, the trace information of covariance matrices involved reveals that the RR scheme tends to have a faster convergence speed.

Remark 2. Suppose θ_* is a local minimum, and there exists $r > 0$ such that the stochastic trajectories Θ_t with the starting point $\Theta_0 = \theta_0 \in B(\theta_*, r)$ stay inside the ball $B(\theta_*, r)$ for $t \geq 0$. Also the local strong convexity holds: there exists $c_0 > 0$ such that $(x - y)^\top (\nabla L(x) - \nabla L(y)) \geq c_0 \|x - y\|_2^2$ for $x, y \in B(\theta_*, r)$, then the trajectory driven by (8) converges faster to θ_* compared to the trajectory driven by (6) in the $L^2(0, t; L^2(\mathbb{R}^d))$ -sense.

²We are aware that this approximation might not be valid in many situations. However, this assumption streamlines the SDE analysis.

Let us elaborate the remark 2. We denote the solutions to (6) and (8) as Θ^1 and Θ^2 respectively and compute their convergence rate to the local minimum in $L^2(0, t; L^2(\mathbb{R}^d))$. Consider the function $f(x) = \frac{1}{2}(x - \theta_*)^\top (x - \theta_*)$. By Ito's lemma,

$$df(\Theta_t^i) = \left(-(\Theta_t^i - \theta_*)^\top m(\Theta_t^i) + \frac{\eta}{2} \text{Tr}(\Sigma_i(\Theta_t^i)) \right) dt + (\Theta_t^i - \theta_*)^\top \sigma_i(\Theta_t^i) dW_t$$

for $i = 1, 2$. Therefore, for $i = 1, 2$,

$$\begin{aligned} \mathbb{E}[\|\Theta_t^i - \theta_*\|_2^2] &= \|\theta_0 - \theta_*\|_2^2 + \mathbb{E} \left[\int_0^t \left(-(\Theta_s^i - \theta_*)^\top \nabla L(\Theta_s^i) + \frac{\eta}{2} \text{Tr}(\Sigma_i(\Theta_s^i)) \right) ds \right] \\ &\leq \|\theta_0 - \theta_*\|_2^2 + \frac{\eta}{2} \int_0^t \mathbb{E} [\text{Tr}(\Sigma_i(\Theta_s^i))] ds - c_0 \int_0^t \mathbb{E}[\|\Theta_s^i - \theta_*\|_2^2] ds, \end{aligned}$$

where the last line uses the local strong convexity and $\nabla L(\theta_*) = 0$. Then we deduce that

$$\int_0^t \mathbb{E}[\|\Theta_s^i - \theta_*\|_2^2] ds \leq \int_0^t e^{-c_0(t-s)} \left(\|\theta_0 - \theta_*\|_2^2 + \frac{\eta}{2} \int_0^s \mathbb{E} [\text{Tr}(\Sigma^i(\Theta_\tau^i))] d\tau \right) ds.$$

The direct comparison between two independent stochastic processes is out of our reach, but from above we speculate that in order to obtain a faster convergence to the global minimum, it should have a smaller trace of the covariance matrix. Indeed, by Cauchy-Schwarz, the covariance matrix from (8) has a smaller trace at every small neighborhood of points coinciding with the trajectory from (6) as

$$\begin{aligned} \text{Tr}(\Sigma^2(\Theta_t)) &= \frac{Z(\Theta_t)}{n^2} \sum_{i=1}^n \|\nabla l_i(\Theta_t)\|_2 - \|m(\Theta_t)\|_2^2 \\ &\leq \frac{1}{n} \sum_{i=1}^n \|\nabla l_i(\Theta_t)\|_2^2 - \|m(\Theta_t)\|_2^2 = \text{Tr}(\Sigma^1(\Theta_t)). \end{aligned}$$

Back to the discrete algorithms, it also indicates that the RR scheme (7) improves the convergence rate to a local minimum.

Exit behavior analysis. From a diffusion theory based viewpoint, we explain why compared to the SGD, the RR scheme is less likely to escape the sharp local minimum. We apply the large deviation theory from [6], Chapter 5. Let us use Ω to denote an open, bounded domain containing a unique stable equilibrium point $\theta_* = 0$ so that for $\dot{\phi}_t = -\nabla L(\phi_t)$, for any $\phi_0 \in \Omega$, we have $\phi_t \in \Omega$, $\forall t > 0$ and $\lim_{t \rightarrow \infty} \phi_t = 0$. $\partial\Omega$ can be a separation boundary of two neighboring isolated minima. We use \mathbb{E}_θ to denote expectations with respect to the diffusion process

$$(9) \quad d\Theta_t = -\nabla L(\Theta_t) dt + \sqrt{\eta} \sigma(\Theta_t) dW_t,$$

with $\Theta_0 = \theta$. Let the hitting time be $\tau^\eta := \inf\{t > 0 : \Theta_t \in \partial\Omega\}$, we then introduce

$$(10) \quad u(\theta) = \mathbb{E}_\theta[\tau^\eta].$$

Theorem 5.7.3 in [6] tells that $u(\theta) \in C^2(\Omega) \cap C(\bar{\Omega})$ and is the unique solution of

$$Lu = -1 \quad \text{in } \Omega, \quad u = 0 \quad \text{on } \partial\Omega,$$

where $Lv = \frac{\eta}{2} \sum_{i,j} (\sigma\sigma^\top)_{ij}(\theta) \frac{\partial^2 v}{\partial\theta_i \partial\theta_j} - \nabla L(\theta) \cdot \nabla v$. Define the cost function

$$V(y, z, t) := \inf_{\{\phi \in C[0, t] : \phi_t = z\}} I_y(\phi),$$

where $I_y(\cdot)$ is the good rate function that controls the large deviation principle (LDP) associated with (9), and it has the corresponding formula

$$(11) \quad I_x(\psi) = \begin{cases} \frac{1}{2} \int_0^T \left(\dot{\psi}(t) + \nabla L(\psi(t)) \right)^\top \Sigma^{-1}(\psi(t)) \left(\dot{\psi}(t) + \nabla L(\psi(t)) \right), & \text{if } \psi \in H_1^x([0, T]) \\ +\infty, & \text{if } \psi \notin H_1^x([0, T]), \end{cases}$$

where $H_1^x([0, T]) := \{\psi : \psi(t) = x + \int_0^t \phi(s) ds, \phi \in L^2([0, T])\}$ and $\Sigma = \sigma\sigma^\top$. $V(y, z, t)$ can be interpreted as the cost of forcing the diffusion process (9) to be at the location z at time

t when starting from y . Moreover, by defining $V(y, z) := \int_{t>0} V(y, z, t)$, we have the so-called *quasi-potential* $V(\theta_*, z) = V(0, z)$.

By making the following assumptions

- (1) $\nabla L(\cdot)$ and $\sigma(\cdot)$ are uniformly Lipschitz continuous,
- (2) $\bar{V} := \inf_{z \in \partial\Omega} V(0, z) < +\infty$,
- (3) $\Sigma(\theta)$ is positive definite for $\theta_* = 0$ and uniformly positive definite on $\partial\Omega$,

one can have the precise exponential growth rate of τ^η and the estimate of the mean exit time.

Theorem 2 (Theorem 5.7.11(a), [6]). *With the above assumptions held, for all $\theta \in \Omega$ and any $\delta > 0$,*

$$(12) \quad \lim_{\eta \rightarrow 0} \mathbb{P}_\theta(e^{(\bar{V}+\delta)/\eta} > \tau^\eta > e^{(\bar{V}-\delta)/\eta}) = 1, \quad \text{and} \quad \lim_{\eta \rightarrow 0} \eta \log \mathbb{E}_\theta[\tau^\eta] = \bar{V}.$$

Now let us consider (6) and (8). Since they are in the same time scale and have the same drift, and we learn from Theorem 2 that the exit time depends on \bar{V} , (11) suggests that the comparison is reduced to comparing Σ^1 with Σ^2 . In one dimension, it is straightforward since by Cauchy-Schwarz inequality,

$$\Sigma^2(\psi) = \frac{Z(\psi)}{n^2} \sum_{i=1}^n |\nabla l_i(\psi)| - m(\psi)^2 \leq \frac{1}{n} \sum_{i=1}^n |\nabla l_i(\psi)|^2 - m(\psi)^2 = \Sigma^1(\psi).$$

Therefore, it suggests that for sufficiently small $\eta > 0$, we have $\mathbb{E}_\theta[\tau_1^\eta] \leq \mathbb{E}_\theta[\tau_2^\eta]$. In higher dimensions, unless we compare traces of matrices, it is hard to see directly that $I_{\theta,2}(\psi) \leq I_{\theta,1}(\psi)$. The best we can argue is that (8) has a lower probability to deviate from the gradient flow

$$\dot{\phi}_t = -\nabla L(\phi_t).$$

Lemma 3. *For any $\delta > 0$ and $0 < T < \infty$, we have the inequality*

$$(13) \quad \mathbb{P}_\theta \left(\sup_{t \in [0, T]} |\Theta_t - \phi_t| > \delta \right) \leq \eta c' \mathbb{E}_\theta \left[\int_0^T \text{Tr}(\sigma(\Theta_s) \sigma(\Theta_s)^\top) ds \right],$$

where c' only depends on δ, T and B . This trace bound implies that (8) is closer to ϕ_t with a higher probability.

Lemma 3 indicates that a stochastic gradient flow is close to behave like the gradient flow when the trace of its covariance matrix is small. Here, it implies that the RR scheme is more deterministic compared to SGD. The proof of inequality (13) can be found in the Appendix B.

4. EXPERIMENTS

The analysis above suggests that, for the non-convex optimization problems, the RR scheme is more likely to find the global minimum compared to the vanilla SGD, especially when the global minimum lies in the sharp valley. We empirically verify this in several examples from both data sciences and physical sciences. In particular, we study (1) robust statistics problems under data feature disparities, (2) geometric optimization problems in computational chemistry, and (3) neural network landscape.

4.1. Robust classification/regression. In this example, we consider to use the Welsch loss (see [2]) from robust statistics, where the corresponding loss for each data sample i is

$$(14) \quad l_i(\theta) = 1 - \exp(-(y_i - \theta^\top x_i)^2/2).$$

This loss function has found many applications in regression problems dealing with outliers. Suppose that the goal is to find a global optimizer for a mixed population of multiple subgroups: part of them are quite sensitive in a certain trait, while the rest are much less sensitive in the same trait. In the following two examples, the RR scheme randomly selects the sub-population j with the probability proportional to $a_j \|\nabla l_j(\theta^k)\|_2$ with replacement in each iteration, where a_j denotes the sub-population proportion.

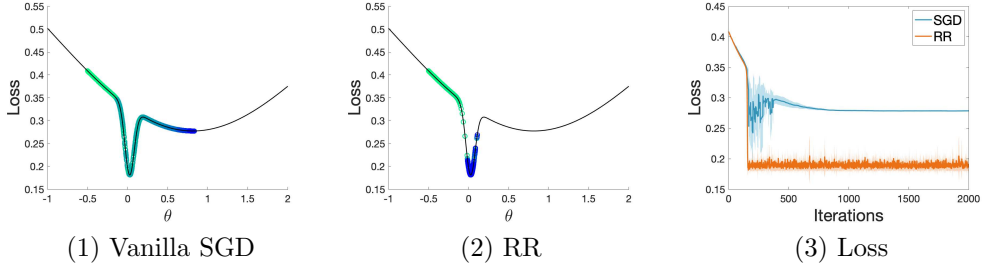


FIGURE 2. We set the starting point $\theta_0 = -0.5$ with a constant learning rate $\eta = 0.015$ in the robust classification problem. The color gradient of circles from green to blue shows how iterations proceed. Plots (1) and (2) show the trajectories for one trial under vanilla SGD and RR, respectively. Plot (3) show the loss comparisons over 10 trials.

Classification. The dataset $\{(x_i, y_i)\}_{1 \leq i \leq N}$, $x_i \in \mathbb{R}$, $y_i \in \{0, 1\}$ consists of x from two subgroups

- Subgroup 1: $x_i = 20 + \mathcal{N}(0, 1)$; total number $N_1 = 800$.
- Subgroup 2: $x_i = 0.5 + \mathcal{N}(0, 1/4)$; total number $N_2 = 4000$.

Here $a_1/a_2 = 1/5$. The class $y_i \sim \text{Ber}(1/2)$ is preassigned for each data point, as we assume that each subgroup contains individuals belonging to different classes. The goal is to find the global minimum rather than a local minimum, even though it is flat. From Fig 2 we can see that in contrast to the vanilla SGD trajectory escapes to the nearby flat local minimum, the RR scheme trajectory stays inside the sharp valley to reach the global minimum.

Regression. The dataset $\{(\mathbf{x}_i, y_i)\}_{1 \leq i \leq N}$, $\mathbf{x}_i \in \mathbb{R}^d$, $d = 10$ is composed of samples from two subgroups

- Subgroup 1: $\mathbf{x}_i = 20\mathbf{e} + \mathcal{N}(0, I_d)$; total number $N_1 = 2000$.
- Subgroup 2: $\mathbf{x}_i = \frac{1}{4}\mathbf{e} + \frac{1}{2}\mathcal{N}(0, I_d)$; total number $N_2 = 800$.

Here $a_1/a_2 = 5/2$. The exact regression coefficient $\beta^* \in \mathbb{R}^d$ is picked by $\beta^* \sim \mathcal{N}(0, I_d)$ and the uncorrupted response variables are $y_i^* = \mathbf{x}_i^\top \beta^*$. The corrupted response variables are generated by $y_i = y_i^* + u_i + \epsilon_i$, where $u_i \sim \text{Unif}([-3\|y^*\|_\infty, 3\|y^*\|_\infty])$, $\epsilon_i \sim \frac{1}{10}\mathcal{N}(0, 1)$. The Fig 3 shows that for a wide range of learning rate choices, the RR scheme selects a better minimum in a faster speed compared to SGD.

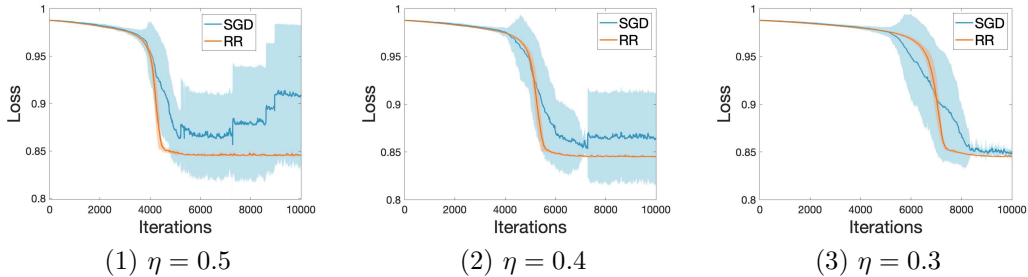


FIGURE 3. Comparisons of the vanilla SGD and the RR scheme for various learning rates over 10 trials in robust regression. For each plot, we start from the same $\beta_0 = \beta^* + 5\mathbf{e} + \epsilon$, $\epsilon \sim \mathcal{N}(0, I_d)$. We observe with a relatively large learning rate, SGD can deviate while the RR scheme is stable around the local minimum. Even when the learning rate decreases and SGD converges to the same minimum that the RR scheme arrives, the convergence speed of SGD is slower.

4.2. Computational chemistry. The problem here is to find the global minimum of a potential energy surface (PES) that typically gives a mathematical description of the molecular structure and its energy. In general, assuming that there are n atoms to form a molecule, we consider minimizing the particle interacting energy of the form

$$E(\mathbf{z}_1, \mathbf{z}_2, \dots, \mathbf{z}_m) = \sum_{i < j}^m V(\mathbf{z}_i, \mathbf{z}_j),$$

where V is a bi-atom potential function, and $\mathbf{z}_k \in \mathbb{R}^d, 1 \leq k \leq m, d \geq 1$ denote the atom's position. In particular, the global minimum represents the most stable conformation with respect to location arrangements of atoms. Though using SGD for a large system is computationally efficient, trying to find the global minimum with SGD can be difficult, especially when the global minimum lies in a sharp valley. The RR scheme outperforms SGD in terms of the likelihood of identifying the global minimum. This is demonstrated in Fig 4 by looking at two examples. The first one is the Müller-Brown potential [17]. The second one is an artificial large system with the interacting function of Gaussian type

$$V_k(\mathbf{z}_i, \mathbf{z}_k) = \exp(-(\mathbf{z}_i - \mathbf{z}_k)^\top M_k (\mathbf{z}_i - \mathbf{z}_k)), \quad M_k = \begin{bmatrix} a_k & b_k/2 \\ b_k/2 & c_k \end{bmatrix},$$

with $\mathbf{z} = (x, y) \in \mathbb{R}^2$. We assume that except for the atom i , the rest of atoms' positions are fixed, then it is to consider minimizing the potential energy $\min_{\mathbf{z}_i} \frac{1}{m-1} \sum_{k \neq i}^m V_k(\mathbf{z}_i, \mathbf{z}_k)$ and finding the optimal \mathbf{z}_i . Detailed parameters setups are provided in the Appendix C.

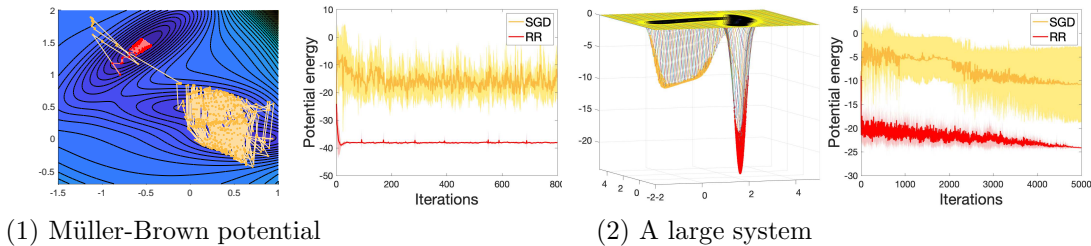


FIGURE 4. (1) The global optimization problem for the 1/4-rescaled Müller-Brown potential with a learning rate $\eta = 0.002$. Both start at $(x_0, y_0) = (-0.8, 1.0)$. (2) A large system with $m = 1000$ atoms in 5000 iterations. Because this problem is rather stiff, we use a monotonically decreasing learning rate starting from $\eta = 0.002$ and ends at $\eta = 1e - 5$ for the optimization. Both trajectories start at $(x_0, y_0) = (3.0, 1.0)$. For both examples (1) and (2), the left plot shows the trajectories for one trial, and the right plot shows the potential energy over 10 trials.

4.3. Neural network landscape. Though the training speed-up of the importance sampling (i.e., the resampling-reweighting scheme) has been studied in the literature, how it selects the minimum has not been fully explored. Here we demonstrate that the importance sampling is more likely to find sharp minima compared to the vanilla SGD in the neural network training. In this example, we consider training a fully connected 3-layer neural network for the MNIST data set ³. For the visualization purpose, we randomly initialize and fix all but two weights. These two weights are updated with the vanilla SGD and the RR scheme. The results shown in Fig 5 are consistent over multiple runs: given the same starting position we set, the RR scheme trajectory goes to the ideal sharp minimum, while the SGD trajectory diverges to the flat nearby local minimum.

³The code was adapted from https://github.com/BundleOfKent/GradientDescentAnimation_NeuralNetwork

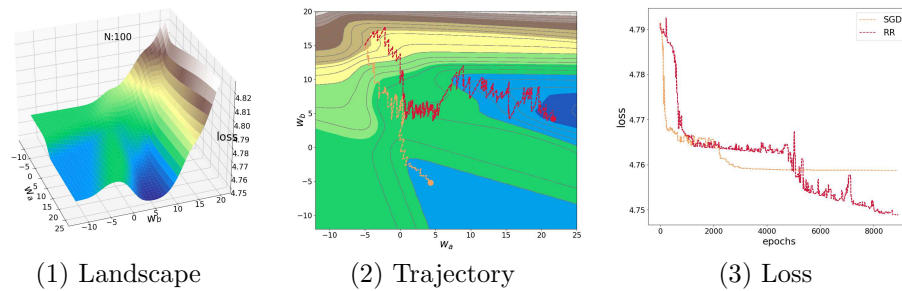


FIGURE 5. Neural network landscape with a learning rate $\eta = 10$. Both start at the same position $(w_a, w_b) = (-5, 15)$, but the trajectories from different algorithms diverge. The RR scheme takes a path to the sharper but also deeper minimum, while the vanilla SGD trajectory goes towards the flatter but shallower neighboring minimum.

REFERENCES

- [1] Guillaume Alain, Alex Lamb, Chinnadhurai Sankar, Aaron Courville, and Yoshua Bengio. Variance reduction in sgd by distributed importance sampling. *arXiv preprint arXiv:1511.06481*, 2015.
- [2] Jonathan T Barron. A general and adaptive robust loss function. In *Proceedings of the IEEE/CVF Conference on Computer Vision and Pattern Recognition*, pages 4331–4339, 2019.
- [3] Olivier Canévet, Cijo Jose, and Francois Fleuret. Importance sampling tree for large-scale empirical expectation. In *International Conference on Machine Learning*, pages 1454–1462. PMLR, 2016.
- [4] Pratik Chaudhari and Stefano Soatto. Stochastic gradient descent performs variational inference, converges to limit cycles for deep networks. In *2018 Information Theory and Applications Workshop (ITA)*, pages 1–10. IEEE, 2018.
- [5] Xiang Cheng, Dong Yin, Peter Bartlett, and Michael Jordan. Stochastic gradient and langevin processes. In *International Conference on Machine Learning*, pages 1810–1819. PMLR, 2020.
- [6] Amir Dembo and Ofer Zeitouni. *Large Deviations Techniques and Applications*. Stochastic Modelling and Applied Probability. Springer Berlin Heidelberg, 2009.
- [7] Elad Hoffer, Itay Hubara, and Daniel Soudry. Train longer, generalize better: closing the generalization gap in large batch training of neural networks. In *Proceedings of the 31st International Conference on Neural Information Processing Systems*, pages 1729–1739, 2017.
- [8] Prateek Jain and Purushottam Kar. Non-convex optimization for machine learning. *Foundations and Trends® in Machine Learning*, 10(3-4):142–336, 2017.
- [9] Tyler B Johnson and Carlos Guestrin. Training deep models faster with robust, approximate importance sampling. *Advances in Neural Information Processing Systems*, 31:7265–7275, 2018.
- [10] Angelos Katharopoulos and François Fleuret. Not all samples are created equal: Deep learning with importance sampling. In *International conference on machine learning*, pages 2525–2534. PMLR, 2018.
- [11] Dmitrii Kochkov and Bryan K Clark. Variational optimization in the ai era: Computational graph states and supervised wave-function optimization. *arXiv preprint arXiv:1811.12423*, 2018.
- [12] Andrew R Leach. *Molecular modelling: principles and applications*. Pearson education, 2001.
- [13] Qianxiao Li, Cheng Tai, and E Weinan. Stochastic modified equations and adaptive stochastic gradient algorithms. In *International Conference on Machine Learning*, pages 2101–2110, 2017.
- [14] Ilya Loshchilov and Frank Hutter. Online batch selection for faster training of neural networks. *arXiv preprint arXiv:1511.06343*, 2015.
- [15] Xingjun Ma, Hanxun Huang, Yisen Wang, Simone Romano, Sarah Erfani, and James Bailey. Normalized loss functions for deep learning with noisy labels. In *International Conference on Machine Learning*, pages 6543–6553. PMLR, 2020.
- [16] Stephan Mandt, Matthew Hoffman, and David Blei. A variational analysis of stochastic gradient algorithms. In *International conference on machine learning*, pages 354–363. PMLR, 2016.
- [17] Klaus Müller and Leo D Brown. Location of saddle points and minimum energy paths by a constrained simplex optimization procedure. *Theoretica chimica acta*, 53(1):75–93, 1979.
- [18] Deanna Needell, Rachel Ward, and Nati Srebro. Stochastic gradient descent, weighted sampling, and the randomized kaczmarz algorithm. *Advances in neural information processing systems*, 27:1017–1025, 2014.
- [19] Peter J Rousseeuw. Least median of squares regression. *Journal of the American statistical association*, 79(388):871–880, 1984.
- [20] Umut Simsekli, Levent Sagun, and Mert Gurbuzbalaban. A tail-index analysis of stochastic gradient noise in deep neural networks. In *International Conference on Machine Learning*, pages 5827–5837. PMLR, 2019.

- [21] Thomas Strohmer and Roman Vershynin. A randomized kaczmarz algorithm with exponential convergence. *Journal of Fourier Analysis and Applications*, 15(2):262–278, 2009.
- [22] Zeke Xie, Issei Sato, and Masashi Sugiyama. A diffusion theory for deep learning dynamics: Stochastic gradient descent escapes from sharp minima exponentially fast. In *International Conference on Learning Representations*, 2021.
- [23] Peilin Zhao and Tong Zhang. Stochastic optimization with importance sampling for regularized loss minimization. In *international conference on machine learning*, pages 1–9. PMLR, 2015.
- [24] Pan Zhou, Jiashi Feng, Chao Ma, Caiming Xiong, Steven Hoi, and Weinan E. Towards theoretically understanding why sgd generalizes better than adam in deep learning. In *Advances in Neural Information Processing Systems*, volume 33, 2020.
- [25] Zhanxing Zhu, Jingfeng Wu, Bing Yu, Lei Wu, and Jinwen Ma. The anisotropic noise in stochastic gradient descent: Its behavior of escaping from minima and regularization effects. In *Proceedings of the 36th International Conference on Machine Learning*, pages 7654–7663, 2019.

APPENDIX A. PROOF OF LEMMA 1

Proof. In different regions, the associated variances are different:

- In regions $(-\infty, -1)$, $(-1, 0)$, $(0, 1/K)$, $(1/K, \infty)$.
- With probability a_1 , the gradients are $-1, 1, \epsilon, \epsilon$ respectively.
- With probability a_2 , the gradients are $-\epsilon, -\epsilon, -K, K$ respectively.
- Corresponding variances are $a_1 a_2 (1 - \epsilon)^2$, $a_1 a_2 (1 + \epsilon)^2$, $a_1 a_2 (K + \epsilon)^2$, $a_1 a_2 (K - \epsilon)^2$ in each region.

Indeed, we take $\epsilon \rightarrow 0$. For $x < 0$, the SGD is approximately

$$(15) \quad \theta \leftarrow \theta - V'(\theta)\eta + \sqrt{a_1 a_2} \eta,$$

and the corresponding SDE is

$$(16) \quad d\Theta_t = -V'(\Theta_t)dt + \sqrt{a_1 a_2} \eta dW_t.$$

For $x > 0$, the SGD is approximately

$$(17) \quad \theta \leftarrow \theta - V'(\theta)\eta + K\sqrt{a_1 a_2} \eta,$$

and the corresponding SDE is

$$(18) \quad d\Theta_t = -V'(\Theta_t)dt + K\sqrt{a_1 a_2} \eta dW_t.$$

The resulted equilibrium measures on two sides are

$$(19) \quad p(\theta) = \frac{1}{Z_1} \exp\left(-\frac{2}{a_1 a_2 \eta} V(\theta)\right) \quad \text{for } \theta < 0, \quad p(\theta) = \frac{1}{Z_2} \exp\left(-\frac{2}{K^2 a_1 a_2 \eta} V(\theta)\right) \quad \text{for } \theta > 0.$$

Consider a SDE with non-smooth diffusion

$$dX_t = \mu(X_t, t)dt + \sigma(X_t, t)dB_t,$$

the corresponding Kolmogorov forward equation is

$$\partial_s p(x, s) = -\partial_x [\mu(x, s)p(x, s)] + \frac{1}{2} \partial_x^2 [\sigma^2(x, s)p(x, s)],$$

for $s \geq t$. For the equilibrium measure $\partial_s p(\theta) = 0$. In order to have $\sigma^2 p$ be continuous at $\theta = 0$, as $V(0) = 0$, it suggests that

$$\frac{1}{Z_1} a_1 a_2 \eta = \frac{1}{Z_2} K^2 a_1 a_2 \eta \quad \implies \quad Z_2 = K^2 Z_1.$$

□

APPENDIX B. PROOF OF LEMMA 3

Proof. Since we assume that ∇L is uniformly Lipschitz continuous, there exists $B > 0$ such that $|\nabla L(x) - \nabla L(y)| \leq B|x - y|$ for all $x, y \in \mathbb{R}^d$. Then we have

$$|\Theta_t - \phi_t| \leq B \int_0^T |\Theta_s - \phi_s| ds + \sqrt{\eta} \left| \int_0^T \sigma(\Theta_s) dW_s \right|.$$

By the Gronwall's inequality, we get

$$\sup_{t \in [0, T]} |\Theta_t - \phi_t| \leq \sqrt{\eta} e^{BT} \sup_{t \in [0, T]} \left| \int_0^T \sigma(\Theta_s) dW_s \right|.$$

Therefore,

$$\begin{aligned}
 \mathbb{P}_\theta \left(\sup_{t \in [0, T]} |\Theta_t - \phi_t| > \delta \right) &\leq \mathbb{P}_\theta \left(\sup_{t \in [0, T]} \left| \int_0^T \sigma(\Theta_s) dW_s \right| > \frac{\delta}{\sqrt{\eta}} e^{-BT} \right) \\
 &\leq \frac{\eta}{\delta^2 e^{-2BT}} \mathbb{E}_\theta \left[\left(\sup_{t \in [0, T]} \left| \int_0^T \sigma(\Theta_s) dW_s \right| \right)^2 \right] \\
 &\leq \eta c' \mathbb{E}_\theta \left[\int_0^T \text{Tr}(\sigma(\Theta_s) \sigma(\Theta_s)^\top) ds \right],
 \end{aligned}$$

where we use Chebyshev's inequality for the second last inequality and Burkholder-Davis-Gundy maximal inequality for the last inequality. \square

APPENDIX C. EXTENDED NUMERICAL RESULTS AND PARAMETERS SETUP

C.1. Numerical comparisons with different learning rates. Here we show more numerical comparisons between SGD and the RR scheme with various learning rates. See Fig 6.

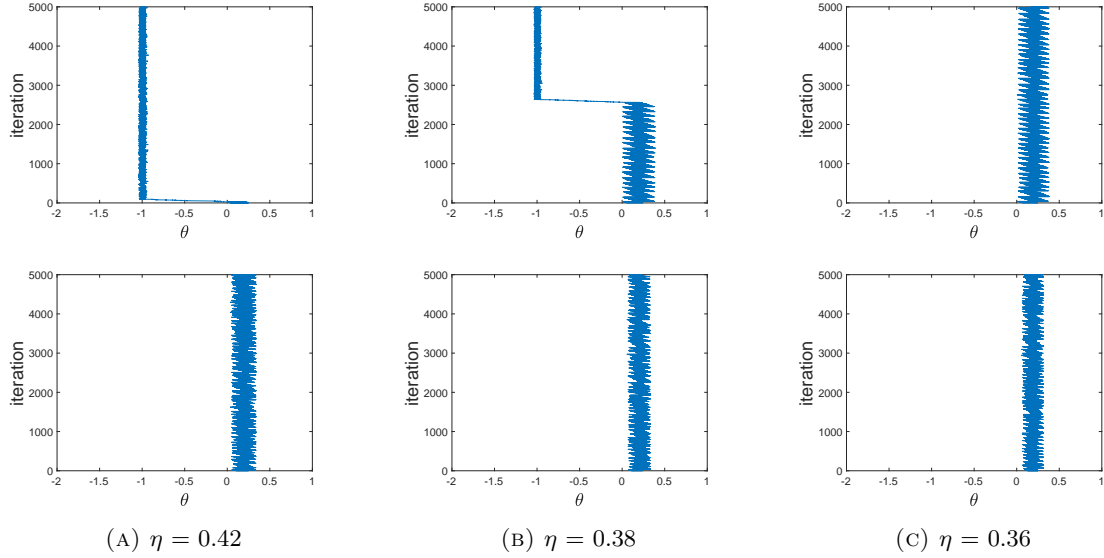


FIGURE 6. Extended comparisons of SGD (upper row) and RR (lower row) with $a_1 = 0.4, a_2 = 0.6, \epsilon = 0.1, K = 5$ at various learning rates η . All experiments start at $\theta_0 = 0.25$. We can see that unless the learning rate $\eta \leq 0.36$, RR is more reliable in the sense that its trajectory stays around the desired minimum. Even when SGD and RR both stay around the sharp global minimum, the oscillation in RR is smaller.

C.2. Parameters setup in Section 4.2.

Müller-Brown potential.

$$\begin{aligned}
 V(x, y) &= \sum_{i=1}^4 A_i \exp \left(a_i (x - x_i)^2 + b_i (x - x_i)(y - y_i) + c_i (y - y_i)^2 \right), \\
 (20) \quad A &= (-150, -100, -170, 15), \quad a = (-1, -1, -6.5, 0.7), \\
 b &= (0, 0, 11, 0.6), \quad c = (-10, -10, -6.5, 0.7), \\
 x &= (1, 0, -0.5, -1), \quad y = (0, 0.5, 1.5, 1).
 \end{aligned}$$

A large system.

$$x_k = 2.0 - 0.006k, 1 \leq k \leq 500, \quad x_k = 1.8 + 0.0024k, 500 \leq k \leq 1000.$$

$$y_k = 2.0 - 0.006k, 1 \leq k \leq 500, \quad y_k = -1.0 + 0.006k, 500 \leq k \leq 1000.$$

$$A_k = -50.0 - 0.15k, a_k = -2.0 - 0.018k, b_k = -0.1 + 0.0002k, c_k = -10 + 0.009k, 1 \leq k \leq 1000.$$

(Jing An) ICME, STANFORD UNIVERSITY, STANFORD, CA 94305

Email address: `jingan@stanford.edu`

(Lexing Ying) DEPARTMENT OF MATHEMATICS AND ICME, STANFORD UNIVERSITY, STANFORD, CA 94305

Email address: `lexing@stanford.edu`